



Cite this: *Phys. Chem. Chem. Phys.*,  
2014, 16, 20030

Received 28th May 2014,  
Accepted 7th August 2014

DOI: 10.1039/c4cp02348j

[www.rsc.org/pccp](http://www.rsc.org/pccp)

## Binding of fullerenes to amyloid beta fibrils: size matters†

Pham Dinh Quoc Huy<sup>a,b</sup> and Mai Suan Li\*<sup>b</sup>

Binding affinity of fullerenes C20, C36, C60, C70 and C84 for amyloid beta fibrils is studied by docking and all-atom molecular dynamics simulations with the Amber 99SB force field and water model TIP3P. Using the molecular mechanic-Poisson Boltzmann surface area method one can demonstrate that the binding free energy linearly decreases with the number of carbon atoms of fullerene, i.e. the larger is the fullerene size, the higher is the binding affinity. Overall, fullerenes bind to A $\beta_{9-40}$  fibrils stronger than to A $\beta_{17-42}$ . The number of water molecules trapped in the interior of 12A $\beta_{9-40}$  fibrils was found to be lower than inside pentamer 5A $\beta_{17-42}$ . C60 destroys A $\beta_{17-42}$  fibril structure to a greater extent compared to other fullerenes. Our study revealed that the van der Waals interaction dominates over the electrostatic interaction and non-polar residues of amyloid beta peptides play the significant role in interaction with fullerenes providing novel insight into the development of drug candidates against Alzheimer's disease.

## 1 Introduction

Alzheimer's disease (AD) is the most common form of dementia among the senior population that increases substantially with the age of the population.<sup>1</sup> AD may be pathologically characterized by progressive intracerebral accumulation of beta amyloid (A $\beta$ ) peptides<sup>2</sup> and  $\tau$ -protein.<sup>3</sup> However, recently accumulated genetic and pathological evidence strongly supports the A $\beta$  cascade hypothesis.<sup>4,5</sup> The A $\beta$  peptides are proteolytic byproduct of the A $\beta$  protein precursor and are most commonly composed of 40 (A $\beta_{40}$ ) and 42 (A $\beta_{42}$ ) amino acids. They appear to be unstructured in their monomer state but aggregate to form fibrils with an ordered cross- $\beta$  sheet pattern.<sup>6-9</sup> Surprisingly, A $\beta$  oligomers are found to be highly toxic to neurons rather than sensible plaques,<sup>10-12</sup> while the A $\beta$  monomer is non-toxic.<sup>13</sup> Therefore, recent approaches to searching for AD drugs have been focused on either blocking, misfolding or disruption of aggregates of A $\beta$  peptides.<sup>4,14</sup> A large number of potential A $\beta$  fibrillogenesis inhibitors have been proposed including polyamines,<sup>15,16</sup> metal chelators,<sup>17</sup>

chaperones,<sup>18</sup> carbohydrate-containing compounds,<sup>19,20</sup> osmolytes,<sup>21</sup> short peptides,<sup>22-26</sup> RNA aptamers<sup>27</sup> and nutraceuticals *etc.*, but none of them have been proved to be efficient for AD treatment.<sup>14,28,29</sup>

Carbon based nanomaterials, such as fullerenes, nanotubes and graphene, have been recently found to interact with and influence assemblies of peptides and proteins.<sup>30</sup> Their applicability and usage in biology and medicine is increasingly being considered, although there is a growing body of literature that alerts to the potential harm to living organisms.<sup>31,32</sup> On the other hand *in vivo* studies showed that fullerene C60 and its derivatives might be non-toxic<sup>33-37</sup> necessitating a deep understanding of the nature of interaction between fullerenes and A $\beta$  fibrils.

Recently, ThT fluorescence measurements of Kim and Lee showed that 1,2-(dimethoxymethano) fullerenes strongly inhibit A $\beta$  peptide aggregation at the early stage<sup>38</sup> generating interest in their potential applications as amyloid pathway blockers or amyloid destabilizes. It has been shown by transmission electron microscopy that the hydrated fullerene (C60:(H<sub>2</sub>O)<sub>n</sub>) inhibited the fibrillization of the A $\beta_{25-35}$  peptide.<sup>39</sup> More complicated derivatives of fullerenes such as [C60Cl(C<sub>6</sub>H<sub>4</sub>CH<sub>2</sub>C)Na], Na<sub>4</sub>[C60(OH)<sub>30</sub>] and the complexes of fullerenes with polyvinylpyrrolidone were reported to have an inhibitory effect on A $\beta_{1-42}$ .<sup>40-42</sup> Computationally, docking and molecular dynamics (MD) simulations<sup>43</sup> suggested that C60 preferentially binds to the turn region of the hook-like  $\beta$ -sheet, disrupting the A $\beta_{1-42}$  fibril. However, the binding free energy of fullerenes to A $\beta$  fibrils was not estimated and the impact of fullerene size on binding affinity has not been studied either *in silico* or *in vitro*. This problem is important also because the toxicity may be size-dependent. The impact of fullerene size on its binding affinity and capability to degrade

<sup>a</sup> Institute of Computational Science and Technology, Quang Trung Software Center, Ho Chi Minh City, Vietnam

<sup>b</sup> Institute of Physics - Polish Academy of Science, al. Lotników 32/46, 02-668 Warsaw, Poland. E-mail: masli@ifpan.edu.pl

† Electronic supplementary information (ESI) available: Details of molecular dynamics simulations, the list of the most important residues, population of the salt bridge Asp23-Lys28, mean values of fibril contacts, time dependence of RMSD, the interaction energies, the number of fibril contacts and water molecules in the interior of fibrils, the correlation between van der Waals energy and binding free energy, the coordinates of the structures, obtained in the best docking mode for all buckyballs with two targets, and 8 movies on movement of fullerenes in complex with fibrils. See DOI: 10.1039/c4cp02348j

fibrils is not *a priori* clear. On one hand, it seems that a larger fullerene would have more contacts with aggregates leading to the stronger interaction compared to the smaller one. On the other hand, a smaller buckyball has the higher propensity to penetrate into the fibril causing more damage.

In this paper we study the interaction between A $\beta$  fibrils and buckyballs of various sizes including C20, C36, C60, C70 and C84 using the molecular docking and all-atom MD simulations. The smallest fullerene is C20 having the shape of unsaturated dodecahedrane, while the most common fullerene is C60 discovered in 1985.<sup>44</sup> C70, C76, C82 and C84 are produced in nature and hidden in soot. The binding free energy was estimated by the docking and the molecular mechanic-Poisson Boltzmann surface area (MM-PBSA) method, where the all-atom simulations were carried out using the Amber force field 99SB and water model TIP3P. It is shown that the larger is the size of fullerenes the higher is their binding affinity for A $\beta$  fibrils. Overall the fullerene binding to A $\beta_{9-40}$  fibrils is stronger than to A $\beta_{17-42}$ , but some exceptions have been seen. The number of water molecules trapped in the interior of pentamer 5A $\beta_{17-42}$  is larger than inside 12A $\beta_{9-40}$ . Interestingly, C60 was found to be the most prominent in destroying 5A $\beta_{17-42}$  while the size effect is not pronounced in disruption of fibril 12A $\beta_{9-40}$ . The van der Waals (vdW) interaction dominates over the electrostatic interaction as non-polar amino acids are the most active in interaction with fullerenes.

## 2 Materials and methods

### 2.1 Parametrization of C20, C36, C60, C70 and C84

Structures of C20, C36, C60, C70 and C84 are shown in Fig. 1. Their 3D structures are first built up by Gaussview version 5.0<sup>45</sup> then minimized by Gaussian 09<sup>46</sup> with the Hartree–Fock method and basis set 6-31G\*. Software antechamber<sup>47</sup> in the AmberTools package was used to generate their parameters for MD simulations with AMBER99SB<sup>48</sup> and GAFF<sup>49</sup> force fields. ESP charges of fullerenes were taken from the Gaussian output.

### 2.2 Structure of A $\beta_{17-42}$ and A $\beta_{9-40}$ fibrils

The question about polymorphic fibril structures of A $\beta$  peptides is still under hot debate. On one hand, 16 residues of A $\beta_{1-42}$  and 8 residues of A $\beta_{1-40}$  at N-terminal which were believed to be disordered in the fibrillar state were neglected in the construction of fibril structure and a number of fibril models for truncated peptides A $\beta_{17-42}$  and A $\beta_{9-40}$  were proposed.<sup>9,50,51</sup> On the other hand, recent experiments<sup>52–54</sup> have suggested that residues at the N-terminal may be ordered and this terminal could carry some

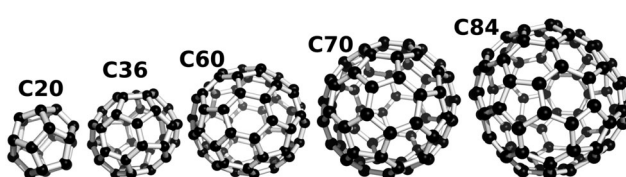


Fig. 1 Structures of C20, C36, C60, C70 and C84.

structural importance. In the fibril model derived from patient brains,<sup>54</sup> for instance, all residues of A $\beta_{1-40}$  are in the fibrillar state. In this paper we performed docking and MD simulations using the fibril structures of five truncated peptides 5A $\beta_{17-42}$  (PDB ID: 2BEG) and 12 truncated peptides 12A $\beta_{9-40}$  (PDB ID: 2LMN).

### 2.3 Docking method

AutodockTools 1.5.4<sup>55</sup> was used to prepare PDBQT files for fibrils of truncated peptides and fullerenes. To dock buckyballs to receptor 5A $\beta_{17-42}$  and 12A $\beta_{9-40}$  PDBQT files were used as the input for the Autodock Vina version 1.1<sup>56</sup> which uses the idea of empirical scoring<sup>57</sup> that the total binding free energy can be separated into several physically distinct contributions. Autodock Vina is approximately two orders of magnitude faster than Autodock 4.<sup>56</sup> This method also significantly improves the accuracy of the binding mode prediction compared with Autodock 4.<sup>56</sup>

A modified version of the CHARMM force field was implemented<sup>58,59</sup> to describe atomic interactions. To obtain accurate results we set the exhaustiveness of global search between 400 and 4000 depending on systems. The maximum energy difference between the worst and best binding modes was set equal to 7. A total 20 binding modes were generated with random starting positions of fullerenes which have fully flexible torsion degrees of freedom. The receptor flexibility is not allowed in our simulations. The center of grids was placed at the center of mass of fibrils. Grid dimensions were chosen large enough to cover the entire fibril.

### 2.4 MD simulations

The Amber11 package<sup>60,61</sup> was used for MD simulation with the AMBER force field 99SB<sup>48</sup> and water model TIP3P<sup>62</sup> which is the best partner for this force field.<sup>63,64</sup> The equations of motion were integrated using a leap-frog algorithm<sup>65</sup> with a time step of 2 fs. The SHAKE algorithm<sup>66</sup> was used to constrain the length of all bonds related to hydrogen atoms. Temperature was controlled using a Langevin thermostat<sup>67</sup> with a collision frequency of 2 ps<sup>-1</sup>. The vdW forces were calculated with a cutoff of 1.4 nm, and the particle mesh Ewald method<sup>68</sup> was employed to treat the long-range electrostatic interactions. The nonbonded interaction pair list, with a cutoff of 1 nm, was updated every 10 fs.

In simulations the structures obtained in the best docking mode were centered in octahedron boxes with periodic boundary conditions. The box sizes and the number of water molecules that occur after solvation are given in Table S1 (ESI<sup>†</sup>). Note that box sizes were chosen large enough to avoid artifacts that may be caused by periodic boundary conditions. Counter ions Na<sup>+</sup> were added to neutralize each system.

### 2.5 MM-PBSA method

The details of the MM-PBSA method are given in our previous studies.<sup>69–71</sup> Overall, in this method the binding free energy of the ligand to the receptor is defined as follows

$$\Delta G_{\text{bind}} = \Delta E_{\text{elec}} + \Delta E_{\text{vdw}} + \Delta G_{\text{sur}} + \Delta G_{\text{PB}} - T\Delta S, \quad (1)$$

where  $\Delta E_{\text{elec}}$  and  $\Delta E_{\text{vdw}}$  are contributions from electrostatic and vdW interactions, respectively.  $\Delta G_{\text{sur}}$  and  $\Delta G_{\text{PB}}$  are non-polar and polar solvation energies. The entropic contribution  $T\Delta S$  is estimated using the normal mode approximation. In order to calculate  $\Delta G_{\text{bind}}$  the MD simulations have been carried out using the Amber 99SB force field and water model TIP3P. The structures of the fibril–fullerene complex obtained in the best docking mode are used as starting configurations for MD simulations. For each system at least a 20 ns to 100 ns MD trajectory was generated (Table S1 in ESI<sup>†</sup>). Snapshots collected in equilibrium are used to compute the binding free energy given by eqn (1).

## 2.6 Tools and measures used in the structure analysis

The time dependence of the number of side chain (SC) contacts was monitored. SC contact is considered as formed if the distance between the nearest fullerene atom and the center of mass of side chain residue is  $<6.5$  Å. The SC contact map is constructed to study the binding process in detail. A salt-bridge (SB) between two charged residues was considered formed if the distance between two specific atoms remains within 4.6 Å. For SB D23–K28 we consider the distance between the C<sup>γ</sup> atom of residue Asp23 and the N<sup>ε</sup> atom of residue Lys28.

## 3 Results and discussion

### 3.1 Docking results

**3.1.1 Aβ fibrils do not have well-defined binding sites.** Here we focus on the results obtained in the best mode which corresponds to the lowest binding energy. In 5Aβ<sub>17–42</sub>, C60 and C20 have the same position near chain A. C20 forms 5 contacts with residues D23-A, G25-A, G29-A, I32-A, and L34-A from chain A (the last letter in the notation like D23-A, for instance, refers to the chain name), and 2 contacts with K28-B and I32-B from chain B (Table 1), while C60 has 7 contacts with chain A and one contact with chain B (Table 1). Totally they share 6 common contacts. C36 instead locates next to chain E of 5Aβ<sub>17–42</sub> with nearest residues F19-E, A21-E, D23-E, L34-E, M35-E, V36-E, and A21-D (Table 1). Similar to C20 and C60, C70 and C84 have the same binding location (Fig. 2) forming 9 and 10 contacts with chains A–D (Table 1) and sharing 9 common contacts. Overall buckyballs are located near the turn region but C20, C36 and C60 are aside, while C70 and C80 are above the layer forming more contacts with the target.

In the case of 12Aβ<sub>9–40</sub>, small balls C20 and C36 are located in the interior of the upper layer (Fig. 3). C60, C70 and C84 are positioned at the same place near the turn region of the

same layer, while C36 is located at the opposite side. C20 has 12 SC contacts with residues from chains A–E, whereas C36 forms 13 contacts mainly with chain A. C60 is bigger than C20 but has the same number of SC contacts (Fig. 3 and Table 2) because the latter is positioned inside the fibril. C60, C70 and C84 share 12 common contacts with the upper layer, but bigger balls C70 and C84 are also in contact with chain L from the lower layer. Since fullerenes locate at different sites, both 5Aβ<sub>17–42</sub> and 12Aβ<sub>9–40</sub> do not possess a well defined binding pocket.

The coordinates of the structures, obtained in the best docking mode for all buckyballs with two targets 5Aβ<sub>17–42</sub> and 12Aβ<sub>9–40</sub>, are supplied in the ESI<sup>1</sup> in the PDB format.

**3.1.2. Binding energy decreases with the number of carbon atoms.** The binding energy varies between  $-5.5$  and  $-8.8$  kcal mol<sup>-1</sup> for 5Aβ<sub>17–42</sub> (Table 1) and  $-8.2$  and  $-16.1$  kcal mol<sup>-1</sup> for 12Aβ<sub>9–40</sub> (Table 2) depending on the ball size. Thus within the docking scheme the binding propensity of fullerene to 12Aβ<sub>9–40</sub> is higher than to 5Aβ<sub>17–42</sub>. However, this result was obtained for fibrils of truncated peptides and its validity for full-length peptides remains to be elucidated.  $\Delta E_{\text{bind}}$  shows a nearly perfect correlation with the size of fullerenes (Fig. 4). This result is understandable because a larger fullerene size would enhance the interaction area leading to higher binding affinity. It should be noted that  $\Delta E_{\text{bind}}$  is not sensitive to the number of SC contacts. C20 and C60, for instance, have the same  $N_{\text{SC}}$  with 12Aβ<sub>9–40</sub> but their binding energies are remarkably different (Table 2). This also holds for C20 and C36 interacting with 5Aβ<sub>17–42</sub> (Table 1). Thus the number of SC alone does not determine the binding affinity of buckyballs to Aβ fibrils.

### 3.2 Molecular dynamics results

The docking method is good for predicting the binding location but its predictive power is limited for estimating the binding energy. Therefore, we will refine the docking results by the MM-PBSA method which is computationally more expensive but more accurate for computation of the binding free energy.

**3.2.1 Equilibration times.** Using the structures obtained in the best docking mode (Fig. 2 and 3), we solvated complexes of fullerene and Aβ fibrils with explicit water. MD simulations, carried out at 300 K, were long enough to generate reasonable sampling in equilibrium. MD simulation details are summarized in Table S1 in the ESI<sup>†</sup>. The duration of MD runs  $\tau_{\text{total}}$  varies between 20 and 100 ns depending on the systems studied.

The equilibration time  $\tau_{\text{eq}}$  may be obtained either from the time dependence of C<sub>α</sub> root mean square displacement (RMSD) of the fibril from its initial structure or from the time dependence of the interaction energy (Fig. S1 and S2 in ESI<sup>†</sup>).  $\tau_{\text{eq}}$ , defined as time

**Table 1** Binding energies  $\Delta E_{\text{bind}}$  (kcal mol<sup>-1</sup>) of fullerenes to 5Aβ<sub>17–42</sub> fibers in the best docking mode.  $N_{\text{SC}}$  is a number of side-chain contacts between the ligand and the receptor. Given is names of amino acids having contact with fullerene, where the last letter refers to the chain of the fibril

	$\Delta E_{\text{bind}}$	$N_{\text{SC}}$	Amino acids that have contact with fullerene
C20	-5.5	7	D23-A, G25-A, G29-A, I32-A, L34-A, K28-B, I32-B
C36	-7.1	7	A21-D, F19-E, A21-E, D23-E, L34-E, M35-E, V36-E
C60	-7.7	8	D23-A, V24-A, G25-A, G29-A, I32-A, G33-A, L34-A, K28-B
C70	-8.2	9	G33-A, M35-A, I31-B, G33-B, M35-B, I31-C, G33-C, M35-C, G-33-D
C80	-8.8	10	G33-A, M35-A, I31-B, G33-B, M35-B, I31-C, G33-C, M35-C, G-33-D, M-35-D

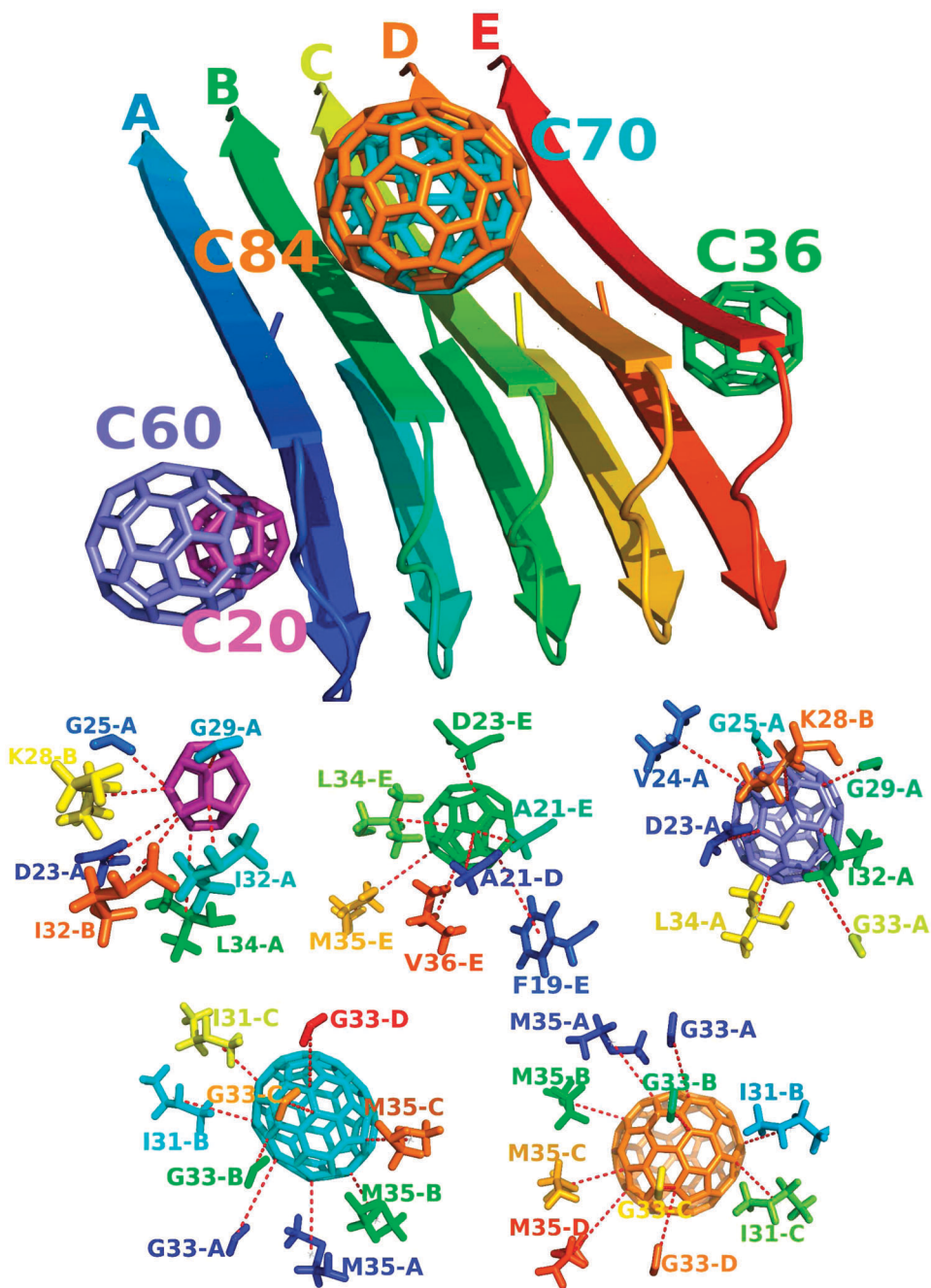


**Fig. 2** Location of fullerenes in the best docking mode in  $5\text{A}\beta_{17-42}$ . Lower plots show side chain contacts. More details of amino acids involved in contact with fullerenes are given in Table 1.

when RMSD saturates and indicated by arrows in Fig. S1 and S2 (ESI†), changes from 3 to 71 ns depending on complexes (Table S1 in ESI†).  $12\text{A}\beta_{9-40}$  without fullerenes reaches equilibrium just after 3 ns while it took 71 ns for the complex  $5\text{A}\beta_{17-42} + \text{C60}$ . Initially C20 located outside  $5\text{A}\beta_{17-42}$ , but during MD simulations it moves inside the fibril and stays there in the equilibrium state having a relatively short equilibration time,  $\tau_{\text{eq}} \approx 17$  ns (see Movie S1 in ESI†). C70 and C84 in complex with  $5\text{A}\beta_{17-42}$  also get equilibrated rapidly as they stay above the layer during simulation (Movie S2 in the ESI†). The situation becomes

very different for C60 which penetrates the fibril affecting its structure to the greatest extent compared to other buckyballs (Movie S3 in ESI†). This explains why the  $5\text{A}\beta_{17-42} + \text{C60}$  complex slowly reaches equilibrium with  $\tau_{\text{eq}} \approx 71$  ns.

Contrary to the  $5\text{A}\beta_{17-42}$  case, the equilibration times for  $12\text{A}\beta_{9-40}$  systems are not very sensitive to fullerene size varying between 7 and 25 ns. This is because the  $12\text{A}\beta_{9-40}$  is a large system and buckyballs mainly fluctuate around the positions predicted by the docking method (see Movie S4 for the  $12\text{A}\beta_{9-40} + \text{C60}$  complex in the ESI†). Finally, fibrils without fullerenes

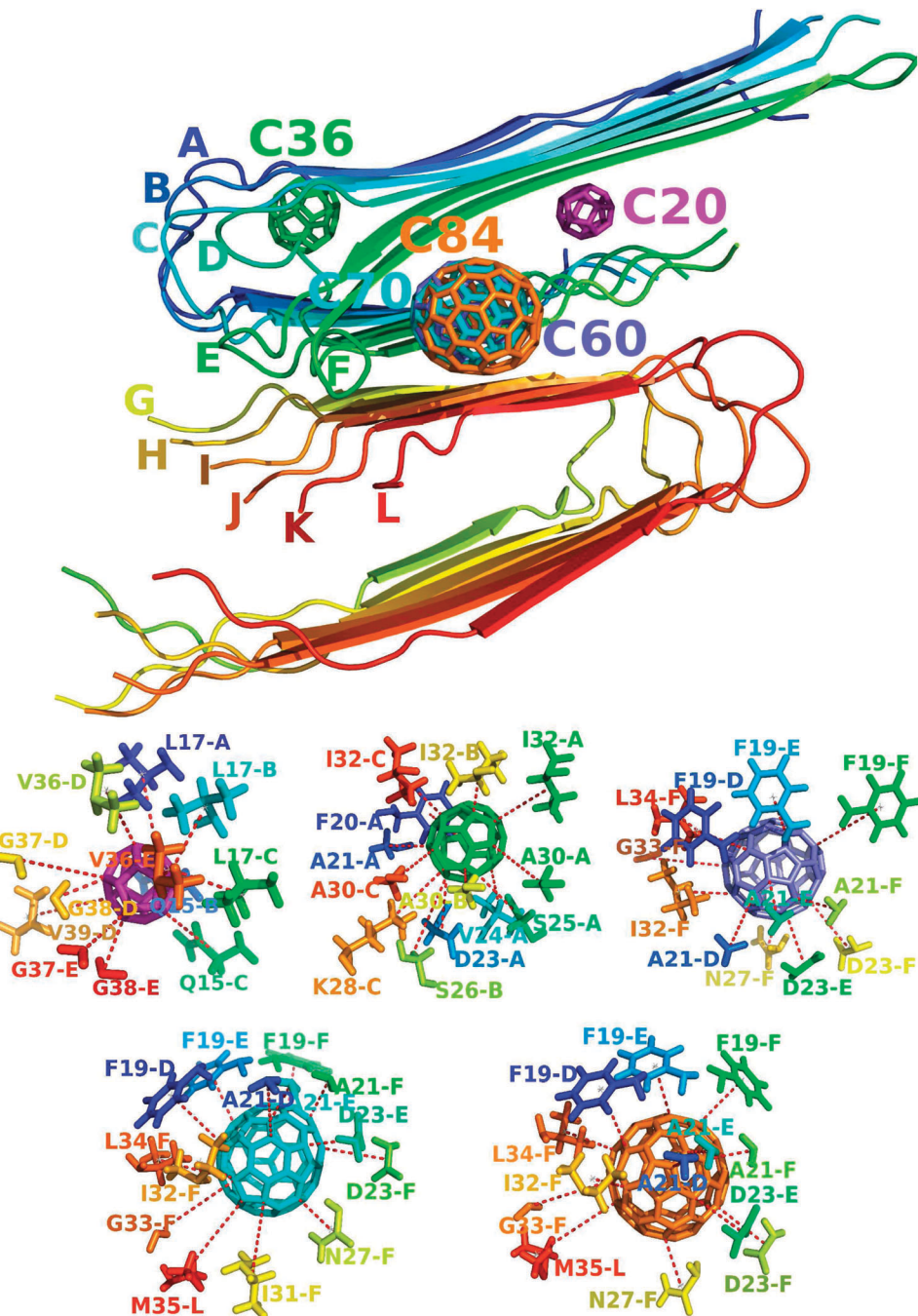


**Fig. 3** Location of fullerenes in the best docking mode in 12A $\beta$ <sub>9–40</sub>. Lower plots show side chain contacts. More details of amino acids involved in contact with fullerenes are given in Table 2.

**Table 2** Binding energy  $\Delta E_{\text{bind}}$  (kcal mol<sup>-1</sup>) of fullerenes to 12A $\beta$ <sub>9–40</sub> in the best docking modes.  $N_{\text{SC}}$  is the number of side-chain contacts. Given is names of amino acids having contact with fullerenes, where the last letter refers to the chain of the fibril

	$\Delta E_{\text{bind}}$	$N_{\text{SC}}$	Amino acids that have contact with fullerene
C <sub>20</sub>	-8.2	12	L17-A, Q15-B, L17-B, Q15-C, L17-C, V36-D, G37-D, G38-D, V39-D, V36-E, G37-E, G38-E
C <sub>36</sub>	-10.4	13	F20-A, A21-A, D23-A, V24-A, S26-A, A30-A, I32-A, S26-B, A30-B, I32-B, K28-C, A30-C, I32-C
C <sub>60</sub>	-13.1	12	F19-D, A21-D, F19-E, A21-E, D23-E, F19-F, A21-F, D23-F, N27-F, I32-F, G33-F, L34-F
C <sub>70</sub>	-14.7	14	F19-D, A21-D, F19-E, A21-E, D23-E, F19-F, A21-F, D23-F, N27-F, I31-F, I32F, G33-F, L34-F, M35-L
C <sub>84</sub>	-16.10	13	F19-D, A21-D, F19-E, A21-E, D23-E, F19-F, A21-F, D23-F, N27-F, I32-F, G33-F, L34-F, M35-L

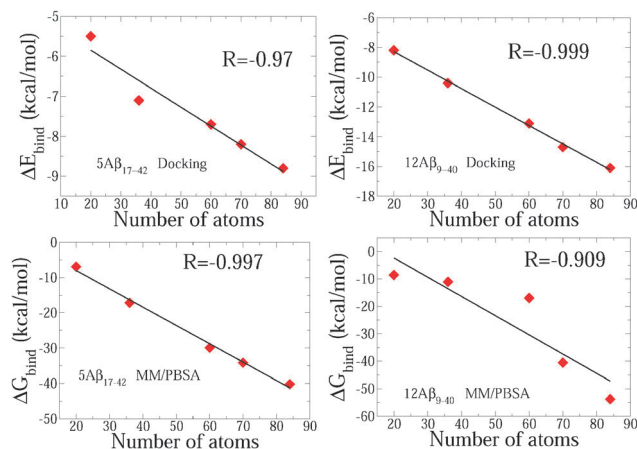


Fig. 4 The correlation between the binding energies and sizes of fullerenes. Upper plots are for docking results, while lower ones are for MM-PBSA.

Table 3 Binding free energy ( $\text{kcal mol}^{-1}$ ) obtained by the MM-PBSA method

Complex	$\Delta E_{\text{vdw}}$	$\Delta E_{\text{elec}}$	$\Delta G_{\text{PB}}$	$\Delta G_{\text{sur}}$	$-T\Delta S$	$\Delta G_{\text{bind}}$
5A $\beta_{17-42}$ + C20	-27.07	-0.71	8.28	-1.35	13.86	<b>-6.99</b>
5A $\beta_{17-42}$ + C36	-40.77	-0.48	12.20	-1.90	13.78	<b>-17.17</b>
5A $\beta_{17-42}$ + C60	-61.73	0.01	20.70	-3.14	14.25	<b>-29.91</b>
5A $\beta_{17-42}$ + C70	-63.53	-0.02	14.12	-3.07	18.34	<b>-34.16</b>
5A $\beta_{17-42}$ + C84	-65.16	-3.05	13.79	-2.61	16.82	<b>-40.21</b>
12A $\beta_{9-40}$ + C20	-30.12	-0.35	8.72	-1.26	14.44	<b>-8.57</b>
12A $\beta_{9-40}$ + C36	-33.14	-0.47	8.03	-1.87	16.40	<b>-11.05</b>
12A $\beta_{9-40}$ + C60	-49.74	-0.04	11.83	-2.70	23.67	<b>-16.98</b>
12A $\beta_{9-40}$ + C70	-83.91	-0.10	24.53	-3.75	22.69	<b>-40.54</b>
12A $\beta_{9-40}$ + C84	-93.42	-2.59	28.75	-4.22	17.73	<b>-53.75</b>

equilibrate faster than systems with buckyballs (Fig. S2 and Table S1 in the ESI†).

**3.2.2 Estimation of  $\Delta G_{\text{bind}}$  by the MM-PBSA method.** Snapshots collected every 10 ps after equilibration are used for estimation of the binding free energy by the MM-PBSA method. The binding free energies and their decomposed parts are given in Table 3 for all systems. For 5A $\beta_{17-42}$   $\Delta G_{\text{bind}}$  varies between  $-6.9$  and  $-34.2$   $\text{kcal mol}^{-1}$  depending on fullerene sizes. The range of its variation is wider for 12A $\beta_{9-40}$  (between  $-8.6$  and  $-53.7$   $\text{kcal mol}^{-1}$ ) but this does not mean that all buckyballs bind to 12A $\beta_{9-40}$  stronger than to 5A $\beta_{17-42}$ . The binding affinity of C36 and C60 for 12A $\beta_{9-40}$  is even lower than for 5A $\beta_{17-42}$ . C60 interacts with 5A $\beta_{17-42}$  stronger than with 12A $\beta_{9-40}$  because, as mentioned above, it can move inside interacting with more chains (compare Movies S3 and S4, ESI†). C36 mainly fluctuates near the central hydrophobic core A $\beta_{17-22}$  of 5A $\beta_{17-42}$  (Movie S5 in ESI†) leading to the interaction stronger than with 12A $\beta_{9-40}$ , where it preferably stays in the turn region (Movie S6 in ESI†).

Although the docking and MM-PBSA methods have quite different scoring functions, they provide the same qualitative result that the bigger is the size of the fullerene the stronger its binding affinity for A $\beta$  fibrils (Fig. 4). The correlation between  $\Delta G_{\text{bind}}$  and the number of carbon atoms of fullerenes is

0.997 and 0.909 for 5A $\beta_{17-42}$  and 12A $\beta_{9-40}$ , respectively. The strong binding of C60 to both targets is qualitatively consistent with experiments<sup>38–42</sup> and prior simulations.<sup>43</sup> The binding affinity of C36 and C60 for 12A $\beta_{9-40}$  is compatible to that of curcumin. Namely, using the MM-PBSA method and the Gromos force field<sup>96</sup> 43a1 it was found that  $\Delta G_{\text{bind}} \approx -13.5 \text{ kcal mol}^{-1}$  for binding of curcumin to 6A $\beta_{9-42}$ .<sup>72</sup> Except C20 which has relatively low binding propensity buckyballs are good in interfering with activity of A $\beta$  peptides.

Because fullerenes consist of only carbon atoms with high symmetry properties, their charges are small (Table S1 in ESI†) leading to the minor electrostatic contribution to  $\Delta G_{\text{bind}}$ . In contrast, the vdW contribution dominates having a high correlation with  $\Delta G_{\text{bind}}$  (see Fig. S3 in ESI†). The nonpolar solvation energy  $\Delta G_{\text{sur}}$  is not sensitive to fullerene size and much less compared to the polar term  $\Delta G_{\text{PB}}$ . The inequality  $|\Delta G_{\text{PB}}| > |\Delta G_{\text{sur}}|$  is valid not only for fullerenes but also for other small compounds<sup>72,73</sup> and short peptides<sup>74</sup> binding to A $\beta$  fibrils.

**3.2.3 Nonpolar amino acids play a key role in fullerene-A $\beta$  interaction.** In order to shed more light on the nature of fullerene binding to A $\beta$  fibrils we monitored the time dependence of SC contacts between the buckyball and each residue of fibrils. Fig. 5 shows the percentage of time during which amino acids form SC contact with fullerene in equilibrium. For 5A $\beta_{17-42}$ , C20 has contact with chains A, B and C, while C60 interacts intensively with chains A and B. C36 forms contacts with chains B, C, D and E, whereas all 5 chains interact with C70 and C84 probably because these balls are big. In 12A $\beta_{9-40}$ , C20 and C36 interact with chains from the first layer, while bigger balls C60, C70 and C84 have contacts with chains from both layers.

Assuming that the most important residues are those residues that have the population exceeding 50% (see Fig. 5), we obtained the full list of such residues shown in Table S2 in the ESI†. In 5A $\beta_{17-42}$  small balls C20, C36 and C60 interact with non-polar and polar residues but C70 and C84 interact with nonpolar residues only. In the case of 12A $\beta_{9-40}$  C60 interacts with non-polar residues from two layers, while the remaining fullerenes also interact with polar amino acids. Overall, the interaction of fullerenes with non-polar residues is dominating.

Having used the ThT fluorescence assay, Kim and Lee reported that 1,2-(dimethoxymethano) fullerene C60 specifically binds to the central hydrophobic motif, KLVFF (amino acids 16–22) of A $\beta_{40}$  monomers.<sup>38</sup> Our simulation shows that, in qualitative agreement with this finding, C60 strongly interacts with F19 from chain D and L17 and F19 from chain F of 12A $\beta_{9-40}$  (Fig. 5).

**3.2.4 Impact of fullerene on salt bridge D23–K28.** Previous computational<sup>75–77</sup> and experimental studies<sup>78</sup> revealed the important role of the salt bridge D23–K28 in the fibril formation process. The formation of a lactam bridge connecting residues 23 and 28 suppresses the lag phase prior to A $\beta_{40}$  nucleation.<sup>78</sup> We have estimated the life time of intra-chain SB D23–K28 in equilibrium for all systems (Tables S3 and S4 in ESI†). In the absence of fullerene the SB of chains B–E of 5A $\beta_{17-42}$  exists during the entire equilibrium period against the population of 45.4% of SB from chain A. The life time of SB D23–K28 of

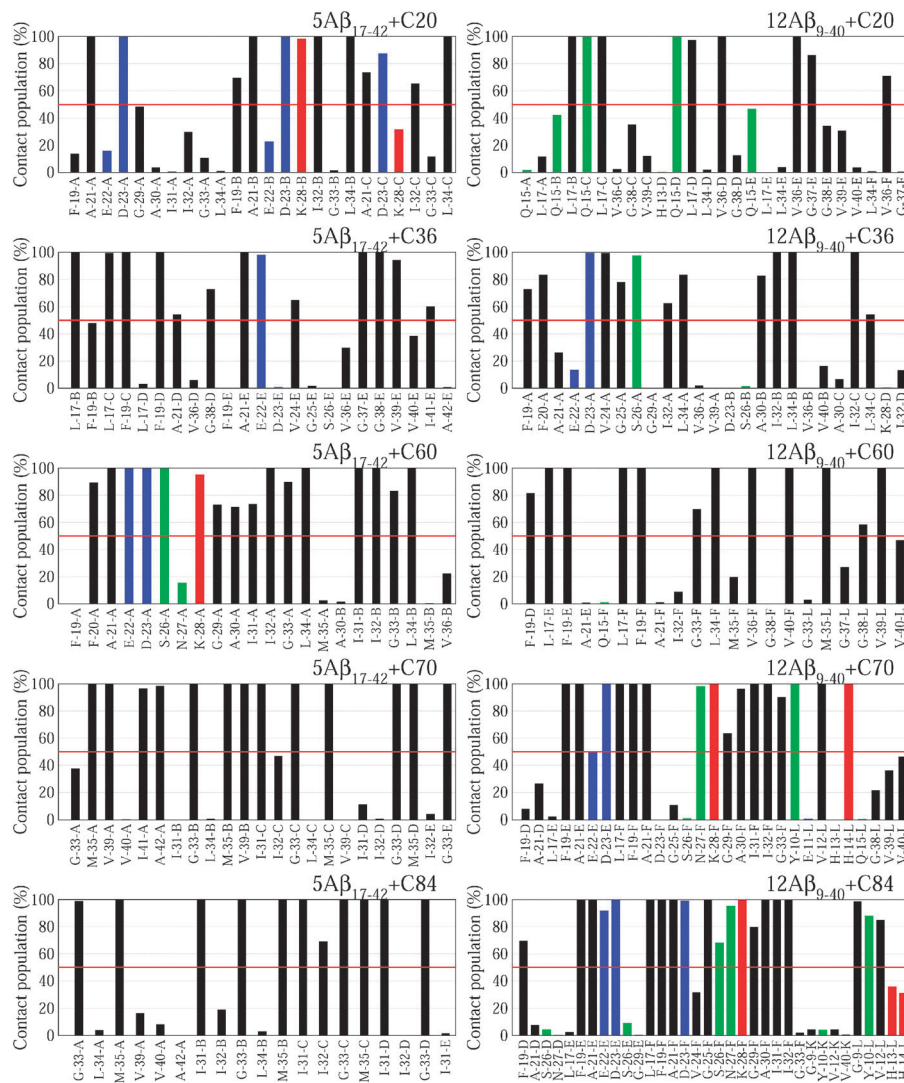


**Fig. 5** Portion of time during which amino acids form contact with fullerenes. Amino acids which make contact more than 50% are the most relevant for binding affinity. Table S2 in the ESI† provides the list of the most important amino acids.

chain A sharply drops to zero in the presence of fullerenes leaving SB from chains B, C and D unaffected. The SB population of chains E is strongly influenced by C36 and C60 but not by other fullerenes. Thus, fullerenes may degrade the 5A $\beta_{17-42}$  fibril through destabilizing D23-K28 SB.

Contrary to the 5A $\beta_{17-42}$  case, SB of chain G in the lower layer of 12A $\beta_{9-40}$  is stable (Table S4 in ESI†) and it is poorly populated in chain A. In the presence of C20, C36 and C70 none of the SBs remains stable, while C60 and C84 stabilize SB from chain L and B, respectively. Overall, the fullerenes destabilize 12A $\beta_{9-40}$  to a lesser extent compared to 5A $\beta_{17-42}$ .

### 3.2.5 Impact of fullerene on evolution of fibril contacts.

The  $\beta$ -sheet structure of the A $\beta$  fibril is stabilized by fibril contacts (FC) between side chains of residues from two neighboring chains. Therefore, to study the influence of fullerenes on stability of fibril structure, we monitor the number of FCs as a function of time. Without fullerenes the PDB structures of 5A $\beta_{17-42}$  and 12A $\beta_{9-40}$  have, correspondingly, 161 and 503 FCs.

As evident from Fig. S2 (ESI†), in equilibrium C $\alpha$  RMSD of both fibrils exceeds 3 Å suggesting that the PDB structures are not very stable at least within the force field Amber 99SB and water model TIP3P. For this reason the number of FCs drops quickly at the early stage and then keeps decreasing until the system gets equilibrated (Fig. S4 and S5 in ESI†). The mean value of FCs in equilibrium is about 100 for 5A $\beta_{17-42}$  and 325 for 12A $\beta_{9-40}$  (Table S5 in ESI†), i.e. only about 60% of initial PDB FCs survive (Fig. 6).

The size of fullerenes affects the stability of 5A $\beta_{17-42}$  in a non-trivial way (Fig. 6). C20, C36 and C70 do not change FCs while C84 even slightly stabilizes the system. The impact of C60 is the most remarkable as in its presence only 45% FCs survive (Table S5 in ESI† and Fig. 6). This interesting effect may be explained as follows. All of the small buckyballs C20, C36 and C60 can penetrate into fibrils but C60 deforms A $\beta$  structure to a larger extent compared to C20 and C36 due to its largest size (Movie S3 in ESI†). On the other hand, big balls C70 and C84

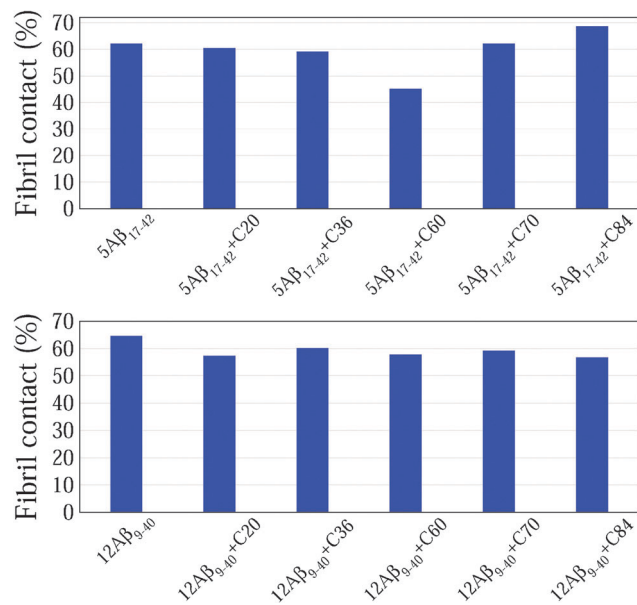


Fig. 6 Mean number of fibril contacts for the equilibration period. See Table S5 in the ESI† for information about their values.

move only around  $5\text{A}\beta_{17-42}$  causing less damage to fibril structure than C60. Taken together the size of C60 is critical for  $5\text{A}\beta_{17-42}$  stability and this is consistent with the prior simulations<sup>43</sup> showing that C60 substantially disrupts the  $\text{A}\beta_{42}$  fibril.

In  $12\text{A}\beta_{9-40}$  fullerenes only reduce FCs by a few percents (Fig. 6) and the fibril stability is, therefore, mainly affected by thermal fluctuations. The size effect is not so pronounced as in the case of  $5\text{A}\beta_{17-42}$  because C60 only moves around  $12\text{A}\beta_{9-40}$  (Movie S4 in ESI†).

**3.2.6  $5\text{A}\beta_{17-42}$  accommodates more water molecules inside than  $12\text{A}\beta_{9-40}$ .** It has long been appreciated that water play a major role in the self-assembly of proteins as hydrophobic residues are predominantly sequestered in protein interior.<sup>79</sup> However, the effects of water on protein aggregation are poorly understood. This is because of experimental difficulties in directly monitoring water activity during the growth process and limitation of computer simulation which is restricted to

time scales much shorter than fibril formation times. Here we study the impact of fullerenes on the number of water molecules inside of  $5\text{A}\beta_{17-42}$  and  $12\text{A}\beta_{9-40}$  and in the area between two layers of  $12\text{A}\beta_{9-40}$ . Just after solvation and minimization steps, no water present in the fibril interior as well as in the area between two layers of  $12\text{A}\beta_{9-40}$ . Because those regions are narrow and largely hydrophobic, thermal fluctuations allow water molecules to move in only after the system was heated up (Fig. 7). The time dependence of water molecules inside  $5\text{A}\beta_{17-42}$  and  $12\text{A}\beta_{9-40}$  and their complexes with fullerenes is shown in Fig. S5 in the ESI†. In the absence of fullerene the interior of  $5\text{A}\beta_{17-42}$  is hydrated to a greater extent compared to  $12\text{A}\beta_{9-40}$  (black bars in Fig. 8). This remains valid in the presence of fullerenes suggesting that the weaker fullerene binding to  $5\text{A}\beta_{17-42}$  is caused by the stronger screening effect by water.

In equilibrium C20, C36 and C60 enhance hydration inside  $5\text{A}\beta_{17-42}$  increasing the number of water molecules  $N_{\text{wt}}$  from about 21 to 26, 29, and 35. The most pronounced enhancement was observed for C60 damaging, as discussed above, the fibril structure to the greatest extent. The fluctuation of  $N_{\text{wt}}$  is also strongest for the  $5\text{A}\beta_{17-42} + \text{C60}$  complex as evident from Fig. S5 in the ESI†. In contrast, C70 and C84 caused only small fluctuations in  $N_{\text{wt}}$  slightly expelling water to the bulk of  $5\text{A}\beta_{17-42}$  (Fig. 8). The correlation between the binding free energy and  $N_{\text{wt}}$  in the interior of  $5\text{A}\beta_{17-42}$  is rather weak ( $R = 0.48$ , Fig. 9) presumably because C20, C36 and C60 reside inside, while C70 and C84 outside the fibril.

In the absence of fullerene water molecules in layer 1 and in the interlayer area (ILA) of  $12\text{A}\beta_{9-40}$  are less than in layer 2 (Fig. 8 and Fig. S5 in ESI†). Because C20 and C36 reside in the interior of the layer 1 (Movies S5 and S6, ESI†) they have a minor impact on hydration of the ILA. C36, C70 and C84 increase  $N_{\text{wt}}$  in this area moving around it (Movies S4, S7 and S8, ESI†). Interestingly, the binding free energy is highly correlated with  $N_{\text{wt}}$  in the interlayer space ( $R = 0.94$ , Fig. 9) in such a way that the hydration enhances the binding affinity of fullerene. This is because big fullerenes interact with two layers of  $12\text{A}\beta_{9-40}$  stronger than small ones letting more water molecules to locate between them.

Fullerenes have a similar impact on water content inside  $5\text{A}\beta_{17-42}$  and layer 1 of  $12\text{A}\beta_{9-40}$  (Fig. 8). Although C60 does not

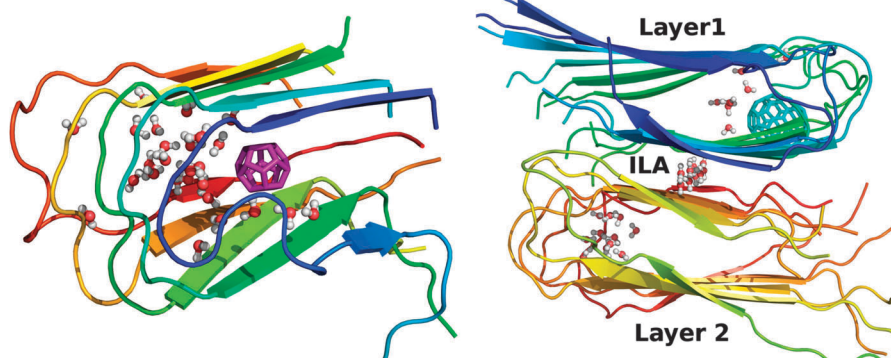


Fig. 7 Representative plots showing water molecules inside the fibril and in the ILA of  $12\text{A}\beta_{9-40}$ .

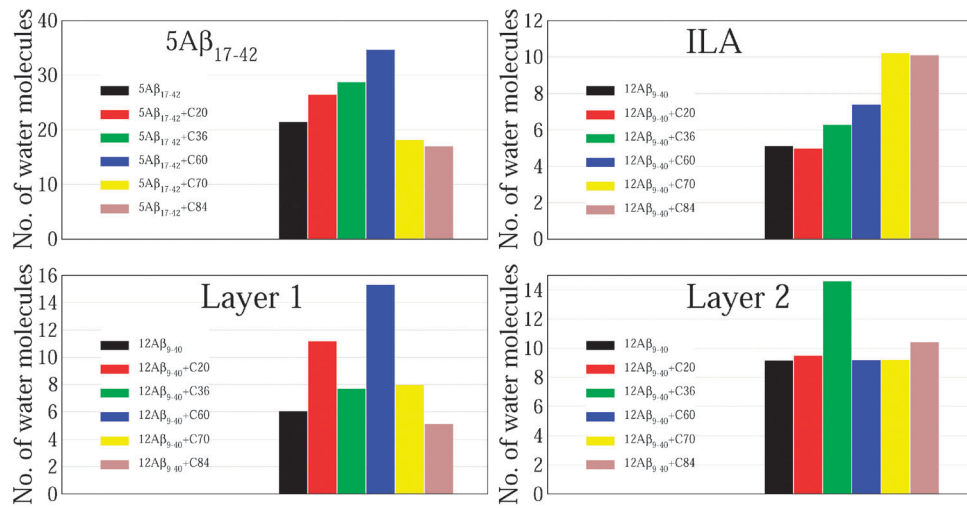


Fig. 8 Mean number of water molecules in the interior of 5A $\beta_{17-42}$  and 12A $\beta_{9-40}$  and in the interlayer area of 12A $\beta_{9-40}$ . Results were obtained in equilibrium.

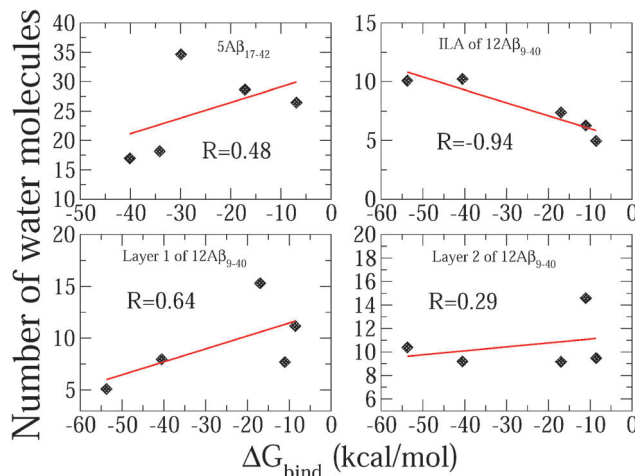


Fig. 9 Correlation between the number of water molecules inside the fibril and  $\Delta G_{bind}$ . Results were obtained in equilibrium.

deeply penetrate into the fibril as in the case of 5A $\beta_{17-42}$  + C60, it considerably affects the structure of layer 1 (Movie S4, ESI<sup>†</sup>) allowing water molecules move in to a greater extent than other fullerenes. The correlation between  $\Delta G_{bind}$  and  $N_{wt}$  inside layer 1 is higher than in the 5A $\beta_{17-42}$  case ( $R = 0.64$  versus  $R = 0.48$ , Fig. 8) because all buckyballs directly interact with water in this area. For layer 2, the number of water molecules of all systems including the case of 12A $\beta_{9-40}$  alone are nearly the same indicating that the presence of fullerenes is not important as fullerenes are located far away from it. As a result, there is no correlation between  $\Delta G_{bind}$  and  $N_{wt}$  in the interior of this layer (Fig. 8).

The question about the existence of water in the interior of the fibril is still under debate.<sup>80</sup> Since fibrillogenic proteins are highly hydrophobic water molecules are expected to be exposed to the bulk making the interior area between  $\beta$ -sheets dry. Computationally, the full as well as partial dewetting was reported for a number of short peptides.<sup>81,82</sup> Formation of

water channels near salt-bridge D23-K28 was observed in simulations of a solid-state NMR-derived structure of the A $\beta_{9-40}$  fibril.<sup>83</sup> Using 2D IR spectroscopy Kim *et al.* have provided evidence for mobile water molecules in A $\beta_{1-40}$  fibrils.<sup>84</sup> Thus, our results are qualitatively consistent with prior simulations<sup>83</sup> and experiments.

## 4 Conclusion

For the first time we have studied the size effect on binding affinity of fullerene buckyballs for A $\beta$  fibrils using the docking and all-atom MD simulations in explicit solvent. Our main findings can be summarized as follows.

In qualitative agreement with experiments we showed that C60 strongly binds to A $\beta$  fibrils. The binding free energy was found to linearly decrease with the size of fullerenes but their capability in destroying A $\beta$  aggregates presumably depends on size in a non-trivial way. Namely, C60 is the most prominent in disrupting pentamer 5A $\beta_{17-42}$  but not C84, whereas the size effect is not pronounced in the case of 12A $\beta_{9-40}$ . It would be interesting to see if this conclusion holds for larger fibers but this question is beyond the scope of the present paper.

We found that the contribution of the van der Waals interaction dominates over the electrostatic interaction as fullerene buckyballs are neutral objects and nonpolar residues are the most active in A $\beta$ -fullerene interaction. Since most of the residues of A $\beta$  sequences are hydrophobic the interior of the fibril is expected to be dry. However, it was found that more water molecules trapped inside 5A $\beta_{17-42}$  than in the interior of one layer of 12A $\beta_{9-40}$ . A structure with trapped water molecules is probably in the metastable state and is one of the polymorphic fibril structures that depend on incubation conditions. Our finding is in line with prior simulations<sup>83</sup> as well as with the experiment of Kim *et al.*<sup>84</sup> For the 5A $\beta_{17-42}$  the correlation between the number of water molecules inside the fibril and  $\Delta G_{bind}$  is poor because the balls are located outside.

In 12A $\beta_{9-40}$  one observed the high impact of water molecules located in the ILA on the binding affinity.

Recently, functionized fullerenes which are soluble in water<sup>85,86</sup> and fullerene assemblies<sup>87,88</sup> have attracted a lot of attention of researchers as they may have important applications in biology and medicine. Therefore, it would be of great interest to study the impact of such fullerene-based compounds on amyloid aggregation.

## Acknowledgements

This work was supported by Narodowe Centrum Nauki in Poland (grant No. 2011/01/B/NZ1/01622), Vietnam National Foundation for Science and Technology Development (NAFOSTED) under grant number 106-YS.02-2013.01 and Department of Science and Technology at Ho Chi Minh city, Vietnam. Allocation of CPU time at the supercomputer center TASK in Gdansk (Poland) is highly appreciated.

## References

- 1 A. S. Henderson and A. F. Jorm, *Dementia*, John Wiley & Sons Ltd, 2002.
- 2 J. Hardy and D. J. Selkoe, *Science*, 2002, **297**, 353–356.
- 3 A. Alonso, T. Zaidi, M. Novak, I. Grundke-Iqbali and K. Iqbali, *Proc. Natl. Acad. Sci. U. S. A.*, 2001, **98**, 6923–6928.
- 4 M. Citron, *Nat. Rev. Neurosci.*, 2004, **5**, 677–685.
- 5 A. Aguzzi and T. O'Connor, *Nat. Rev. Drug Discovery*, 2010, **9**, 237–248.
- 6 E. D. Eanes and G. G. Glenner, *J. Histochem. Cytochem.*, 1968, **16**, 673–677.
- 7 D. A. Kirschner, C. Abraham and D. J. Selkoe, *Proc. Natl. Acad. Sci. U. S. A.*, 1986, **83**, 503–507.
- 8 A. T. Petkova, Y. Ishii, J. J. Balbach, O. N. Antzutkin, R. D. Leapman, F. Delaglio and R. Tycko, *Proc. Natl. Acad. Sci. U. S. A.*, 2002, **99**, 16742–16747.
- 9 T. Luhrs, C. Ritter, M. Adrian, D. Riek-Lohr, B. Bohrmann, H. Dobeli, D. Schubert and R. Riek, *Proc. Natl. Acad. Sci. U. S. A.*, 2005, **102**, 17342–17347.
- 10 A. E. Roher, M. O. Chaney, Y. M. Kuo, S. D. Webster, W. B. Stine, L. J. Haverkamp, A. S. Woods, R. J. Cotter, J. M. Tuohy, G. A. Krafft, B. S. Bonnell and M. R. Emmerling, *J. Biol. Chem.*, 1996, **271**, 20631–20635.
- 11 M. Townsend, G. M. Shankar, T. Mehta, D. M. Walsh and D. J. Selkoe, *J. Physiol.*, 2006, **572**, 477–492.
- 12 S. Lesne, M. T. Koh, L. Kotilinek, R. Kayed, C. G. Glabe, A. Yang, M. Gallagher and K. H. Ashe, *Nature*, 2006, **440**, 352–357.
- 13 K. N. Dahlgren, A. M. Manelli, W. B. Stine, L. K. Baker, G. A. Krafft and M. J. LaDu, *J. Biol. Chem.*, 2002, **277**, 32046–32053.
- 14 J. L. Cummings, *N. Engl. J. Med.*, 2004, **351**, 56–67.
- 15 S. M. Yatin, M. Yatin, S. Varadarajan, K. B. Ain and D. A. Butterfield, *J. Neurosci. Res.*, 2001, **63**, 395–401.
- 16 G. T. Dolphin, S. Chierici, M. Ouberai, P. Dumy and J. Garcia, *ChemBioChem*, 2008, **9**, 952–963.
- 17 A. I. Bush, *Neurobiol. Aging*, 2002, **23**, 1031–1038.
- 18 C. G. Evans, S. Wisen and J. E. Gestwicki, *J. Biol. Chem.*, 2006, **281**, 33182–33191.
- 19 L. Svennerholm, *Life Sci.*, 1994, **55**, 2125–2134.
- 20 G. M. Castillo, C. Ngo, J. Cummings, T. N. Wight and A. D. Snow, *J. Neurochem.*, 1997, **69**, 2452–2465.
- 21 M. Nitz, D. Fenili, A. A. Darabie, L. Wu, J. E. Cousins and J. McLaurin, *FEBS J.*, 2008, **275**, 1663–1674.
- 22 L. O. Tjernberg, J. Naslund, F. Lindqvist, J. Johansson, A. R. Karlstrom, J. Thyberg, L. Terenius and C. Nordstedt, *J. Biol. Chem.*, 1996, **271**, 8545–8548.
- 23 C. Soto, M. S. Kindy, M. Baumann and B. Frangione, *Biochem. Biophys. Res. Commun.*, 1996, **226**, 672–680.
- 24 C. Adessi and C. Soto, *Drug Dev. Res.*, 2002, **56**, 184–193.
- 25 H. Li, B. H. Monien, A. Lomakin, R. Zemel, E. A. Fradinger, M. Tan, S. M. Spring, B. Urbanc, C. W. Xie, G. B. Benedek and G. Bitan, *Biochemistry*, 2010, **49**, 6358–6364.
- 26 C. Wu, M. M. Murray, S. L. Bernstein, M. M. Condron, G. Bitan, J. E. Shea and M. T. Bowers, *J. Mol. Biol.*, 2009, **387**, 492–501.
- 27 T. Takahashi, K. Tada and H. Mihara, *Mol. BioSyst.*, 2009, **5**, 986–991.
- 28 C. A. Hawkes, V. Ng and J. MacLaurin, *Drug Dev. Res.*, 2009, **70**, 111–124.
- 29 G. Yamin, K. Ono, M. Inayathullah and D. B. Teplow, *Curr. Pharm. Des.*, 2008, **14**, 3231–3246.
- 30 C. Li and R. Mezzenga, *Nanoscale*, 2013, **5**, 6207–6218.
- 31 J. Kayat, V. Gajbhiye, R. K. Tekade and N. K. Jain, *Nanomedicine*, 2011, **7**, 40–49.
- 32 S. T. Yang, Y. Liu, Y. W. Wang and A. N. Cao, *Small*, 2013, **9**, 1635–1653.
- 33 F. Moussa, F. Trivin, R. Ceolin, M. Hadchouel, P. Y. Sizaret, V. Greugny, C. Fabre, A. Rassat and H. Szwarc, *Fullerene Sci. Technol.*, 1996, **4**, 21–29.
- 34 T. Mori, H. Takada, S. Ito, K. Matsubayashi, N. Miwa and T. Sawaguchi, *Toxicology*, 2006, **225**, 48–54.
- 35 N. Gharbi, M. Pressac, M. Hadchouel, H. Szwarc, S. R. Wilson and F. Moussa, *Nano Lett.*, 2005, **5**, 2578–2585.
- 36 J. Kolosnjaj, H. Szwarc and F. Moussa, *Adv. Exp. Med. Biol.*, 2007, **620**, 168–180.
- 37 A. G. Bobylev, A. D. Okuneva, L. G. Bobyleva, I. S. Fadeeva, R. S. Fadeev, N. N. Salmov and Z. A. Poddubnaia, *Biofizika*, 2012, **57**, 746–750.
- 38 J. E. Kim and M. Lee, *Biochem. Biophys. Res. Commun.*, 2003, **303**, 576–579.
- 39 I. Y. Podolski, Z. A. Podlubnaya, E. A. Kosenko, E. A. Mugantseva, E. G. Makarova, L. G. Marsagishvili, M. D. Shpagina, Y. G. Kaminsky, G. V. Andrievsky and V. K. Klochkov, *J. Nanosci. Nanotechnol.*, 2007, **7**, 1479–1485.
- 40 L. G. Marsagishvili, A. G. Bobylev, M. D. Shpagina, P. A. Troshin and Z. A. Podlubnaya, *Biofizika*, 2009, **54**, 202–205.
- 41 A. G. Bobylev, L. G. Marsagishvili, M. D. Shpagina, V. S. Romanova, R. A. Kotel'nikova and Z. A. Podlubnaya, *Biofizika*, 2010, **55**, 394–399.
- 42 A. G. Bobylev, A. B. Kornev, L. G. Bobyleva, M. D. Shpagina, I. S. Fadeeva, R. S. Fadeev, D. G. Deryabin, J. Balzarini,

- P. A. Troshin and Z. A. Podlubnaya, *Org. Biomol. Chem.*, 2011, **9**, 5714–5719.
- 43 S. A. Andujar, F. Lugli, S. Hofinger, R. D. Enriz and F. Zerbetto, *Phys. Chem. Chem. Phys.*, 2012, **14**, 8599–8607.
- 44 H. W. Kroto, J. R. Heath, S. C. O'Brien, R. F. Curl and R. E. Smalley, *Nature*, 1985, **318**, 162–163.
- 45 R. Dennington, T. Keith and J. Millam, *GaussView Version 5*, Semichem Inc., Shawnee Mission KS, 2009.
- 46 M. J. Frisch, G. W. Trucks, H. B. Schlegel, G. E. Scuseria, M. A. Robb, J. R. Cheeseman, G. Scalmani, V. Barone, B. Mennucci, G. A. Petersson, H. Nakatsuji, M. Caricato, X. Li, H. P. Hratchian, A. F. Izmaylov, J. Bloino, G. Zheng, J. L. Sonnenberg, M. Hada, M. Ehara, K. Toyota, R. Fukuda, J. Hasegawa, M. Ishida, T. Nakajima, Y. Honda, O. Kitao, H. Nakai, T. Vreven, J. A. Montgomery, Jr., J. E. Peralta, F. Ogliaro, M. Bearpark, J. J. Heyd, E. Brothers, K. N. Kudin, V. N. Staroverov, R. Kobayashi, J. Normand, K. Raghavachari, A. Rendell, J. C. Burant, S. S. Iyengar, J. Tomasi, M. Cossi, N. Rega, J. M. Millam, M. Klene, J. E. Knox, J. B. Cross, V. Bakken, C. Adamo, J. Jaramillo, R. Gomperts, R. E. Stratmann, O. Yazev, A. J. Austin, R. Cammi, C. Pomelli, J. W. Ochterski, R. L. Martin, K. Morokuma, V. G. Zakrzewski, G. A. Voth, P. Salvador, J. J. Dannenberg, S. Dapprich, A. D. Daniels, Ö. Farkas, J. B. Foresman, J. V. Ortiz, J. Cioslowski and D. J. Fox, *Gaussian 09 Revision D.01*, Gaussian Inc., Wallingford CT, 2009.
- 47 J. Wang, W. Wang, P. A. Kollman and D. A. Case, *J. Mol. Graphics Modell.*, 2006, **25**, 247–260.
- 48 V. Hornak, R. Abel, A. Okur, B. Strockbine, A. Roitberg and C. Simmerling, *Proteins: Struct., Funct., Bioinf.*, 2006, **65**, 712–725.
- 49 J. Wang, R. M. Wolf, J. M. Caldwell, P. A. Kollman and D. A. Case, *J. Comput. Chem.*, 2004, **25**, 1157–1174.
- 50 A. T. Petkova, W.-M. Yau and R. Tycko, *Biochemistry*, 2006, **45**, 498–512.
- 51 A. K. Paravastu, R. D. Leapman, W. M. Yau and R. Tycko, *Proc. Natl. Acad. Sci. U. S. A.*, 2008, **105**, 18349–18354.
- 52 I. Bertini, L. Gonnelli, C. Luchinat, J. Mao and A. Nesi, *J. Am. Chem. Soc.*, 2011, **133**, 16013–16022.
- 53 H. A. Scheidt, I. Morgado, S. Rothemund and D. Huster, *J. Biol. Chem.*, 2012, **287**, 2017–2021.
- 54 J. X. Lu, W. Qiang, W. M. Yau, C. D. Schwieters, S. C. Meredith and R. Tycko, *Cell*, 2013, **154**, 1257–1268.
- 55 M. F. Sanner, *J. Mol. Graphics Modell.*, 1999, **17**, 57–61.
- 56 O. Trott and A. J. Olson, *J. Comput. Chem.*, 2010, **31**, 455–461.
- 57 H. J. Bohm, *J. Comput.-Aided Mol. Des.*, 1994, **8**, 243–256.
- 58 G. M. Morris, D. S. Goodsell, R. S. Halliday, R. Huey, W. E. Hart, R. K. Belew and A. J. Olson, *J. Comput. Chem.*, 1998, **19**, 1639–1662.
- 59 G. M. Morris, D. S. Goodsell, R. Huey and A. J. Olson, *J. Comput.-Aided Mol. Des.*, 1996, **10**, 293–304.
- 60 D. A. Pearlman, D. A. Case, J. W. Caldwell, W. S. Ross, T. E. C. III, S. DeBolt, D. Ferguson, G. Seibel and P. Kollman, *Comput. Phys. Commun.*, 1995, **91**, 1–41.
- 61 D. A. Case, T. E. Cheatham, T. Darden, H. Gohlke, R. Luo, K. M. Merz, A. Onufriev, C. Simmerling, B. Wang and R. J. Woods, *J. Comput. Chem.*, 2005, **26**, 1668–1688.
- 62 W. L. Jorgensen, J. Chandrasekhar, J. D. Madura, R. W. Impey and M. L. Klein, *J. Chem. Phys.*, 1983, **79**, 926–935.
- 63 W. F. van Gunsteren, S. R. Billeter, A. A. Eising, P. H. Hunenberger, P. Kruger, A. E. Mark, W. R. P. Scott and I. G. Tironi, *Biomolecular Simulation: The GROMOS96 Manual and User Guide*, Vdf Hochschulverlag AG an der ETH Zurich, Zurich, 1996.
- 64 T. T. Nguyen, M. H. Viet and M. S. Li, *Sci. World J.*, 2014, **2014**, 36084.
- 65 R. Hockney, S. Goel and J. Eastwood, *J. Comput. Phys.*, 1974, **14**, 148–158.
- 66 J.-P. Ryckaert, G. Cicotti and H. J. Berendsen, *J. Comput. Phys.*, 1977, **23**, 327–341.
- 67 X. W. Wu and B. R. Brooks, *Chem. Phys. Lett.*, 2003, **381**, 512–518.
- 68 T. Darden, D. York and L. Pedersen, *J. Chem. Phys.*, 1993, **98**, 10089–10092.
- 69 T. T. Nguyen, B. K. Mai and M. S. Li, *J. Chem. Inf. Model.*, 2011, **51**, 2266–2276.
- 70 M. H. Viet and M. S. Li, *J. Chem. Phys.*, 2012, **136**, 245105.
- 71 S. T. Ngo and M. S. Li, *J. Phys. Chem. B*, 2012, **116**, 10165–10175.
- 72 S. T. Ngo and M. S. Li, *J. Phys. Chem. B*, 2012, **116**, 10165–10175.
- 73 S. T. Ngo and M. S. Li, *Mol. Simul.*, 2013, **39**, 279–291.
- 74 M. H. Viet, S. T. Ngo, N. S. Lam and M. S. Li, *J. Phys. Chem. B*, 2011, **115**, 7433–7446.
- 75 B. Ma and R. Nussinov, *Proc. Natl. Acad. Sci. U. S. A.*, 2002, **99**, 14126–14131.
- 76 G. Reddy, J. E. Straub and D. Thirumalai, *J. Phys. Chem. B*, 2009, **113**, 1162–1172.
- 77 M. H. Viet, P. H. Nguyen, S. T. Ngo, M. S. Li and P. Derreumaux, *ACS Chem. Neurosci.*, 2013, **4**, 1446–1457.
- 78 K. L. Sciarretta, D. J. Gordon, A. T. Petkova, R. Tycko and S. C. Meredith, *Biochemistry*, 2005, **44**, 6003–6014.
- 79 K. A. Dill, *Biochemistry*, 1990, **29**, 7133–7155.
- 80 D. Thirumalai, G. Reddy and J. E. Straub, *Acc. Chem. Res.*, 2012, **45**, 83–92.
- 81 G. Reddy, J. E. Straub and D. Thirumalai, *Proc. Natl. Acad. Sci. U. S. A.*, 2010, **107**, 21459–21464.
- 82 M. G. Krone, L. Hua, P. Soto, R. H. Zhou, B. J. Berne and J. E. Shea, *J. Am. Chem. Soc.*, 2008, **130**, 11066–11072.
- 83 N. V. Buchete, R. Tycko and G. Hummer, *J. Mol. Biol.*, 2005, **353**, 804–821.
- 84 Y. S. Kim, L. Liu, P. H. Axelsen and R. M. Hochstrasser, *Proc. Natl. Acad. Sci. U. S. A.*, 2009, **106**, 17751–17756.
- 85 E. Nakamura and H. Isobe, *Acc. Chem. Res.*, 2003, **36**, 807–815.
- 86 K. Minami, K. Okamoto, K. Doi, K. Harano, E. Noiri and E. Nakamura, *Sci. Rep.*, 2014, **4**, 4916.
- 87 L. K. Shrestha, Q. Ji, T. Mori, K. Miyazawa, Y. Yamauchi, J. P. Hill and K. Ariga, *Chem. – Asian J.*, 2013, **8**, 1662–1679.
- 88 L. K. Shrestha, M. Sathish, J. P. Hill, K. Miyazawa, T. Tsuruoka, N. M. Sanchez-Ballester, I. Honma, Q. Ji and K. Ariga, *J. Mater. Chem. C*, 2013, **1**, 1174–1181.